Journal of Natural Gas Science and Engineering 21 (2014) 134–146

Contents lists available at ScienceDirect

Journal of Natural Gas Science and Engineering

journal homepage: www.elsevier.com/locate/jngse

A novel integrated thermally double coupled configuration for methane steam reforming, methane oxidation and dehydrogenation of propane

D. Karimipourfard [a], S. Kabiri [a], M.R. Rahimpour [a, b, *]

[a] Department of Chemical Engineering, School of Chemical and Petroleum Engineering, Shiraz University, Shiraz 71345, Iran
[b] Gas Center of Excellence, Shiraz University, Shiraz 71345, Iran

ARTICLE INFO

Article history:
Received 26 March 2014
Received in revised form
22 June 2014
Accepted 23 June 2014
Available online 23 August 2014

Keywords:
Thermally double coupled reactor
Syngas
Steam reforming
Propane dehydrogenation
Methane oxidation

ABSTRACT

The goal of this study is the simultaneous production of synthesis gas, hydrogen and propylene in a thermally double coupled steam reformer reactor. This reactor has three concentric tubes where the exothermic reaction of methane oxidation is supposed to occur in the middle tube and the inner and outer tubes are considered to be endothermic sides of steam reforming and propane dehydrogenation, respectively. The motivation is to combine the energy efficient concept of coupling one exothermic reaction with two endothermic reactions, enhancement of synthesis gas production, propylene and hydrogen production and also producing two different H_2/CO ratio streams of syngas. A steady state homogeneous model of fixed bed for three sides predicts the performance of this new configuration. The simulation results are compared with corresponding predictions of the conventional steam reformer. The results prove that synthesis gas production is increased in a thermally double coupled reactor in comparison with conventional steam reforming. In addition, the thermally double coupled reactor reduces the capital and operating costs by reducing the reactor size and consumption of energy.

1. Introduction

Nowadays, there has been an enormous increase in energy demands due to fast growing of industrial development and population of the world. The shortage of fossil fuels as a main energy sources has brought energy crisis. In order to eliminate fossil fuel dependence, comprehensive research has been carried out on searching alternative energy resources. Natural gas is recognized as one of the cleanest and most abundant fossil fuels utilized in various industrial processes. Different technologies are today available to convert natural gas to future energy carriers such as synthesis gas of which chemical conversion is of great interest. Conversion increases the value of the raw material 3–10 times (Løvik, 2011). Synthesis gas can be an excellent candidate for future energy carrier due to its high potential energy.

1.1. Synthesis gas

Synthesis gas or syngas is a major route from hydrocarbons to many vital chemical products consisting primarily of H_2 and CO. Syngas can be produced from Natural Gas (NG), refinery off-gases, naphtha, heavy hydrocarbons and also from coal. Hydrogen has been considered as a clean and renewable energy carrier to support energy consumption. Hydrogen has characteristics of an environmentally friendly, efficient, safe and sustainable energy source (Heinzel et al., 2002; Lokurlu et al., 2003). The products of hydrogen combustion are water and a tiny amount of NO_x which can be reduced by proper methods. The use of hydrogen in energy sector enhances the security of energy supply and improves economic competitiveness (Muller-Langer et al., 2007). Hydrogen has the best energy-to-weight ratio of any fuel. A fuel which contains higher proportion of hydrogen provides more energy (Sun et al., 2012). Therefore, pure hydrogen would be the leading fuel, which can satisfy the increasing demand for many processes such as: methanol, electricity, ammonia, aniline, oil refining, fuel cell, vehicle engines, power plants, etc. (Itoh et al., 2008; Brown, 2001). Several processes have been widely investigated as primary processes for

* Corresponding author. Department of Chemical Engineering, School of Chemical and Petroleum Engineering, Shiraz University, Mollasadra Street, Shiraz 71345, Iran. Tel.: +98 711 2303071; fax: +98 711 6287294.
E-mail addresses: rahimpor@shirazu.ac.ir, mrahimpour@ucdavis.edu (M.R. Rahimpour).

http://dx.doi.org/10.1016/j.jngse.2014.06.018
1875-5100/

converting hydrocarbons or alcohols into hydrogen, including steam reforming (Lee and Park, 1998; Ko et al., 1995; Rahimpour and Alizadehhesari, 2009; Rahimpour et al., 2010; Seo et al., 2008a,b; Yu et al., 2009), partial oxidation (Wang et al., 2009; Kim et al., 2004; Gao et al., 2008), auto-thermal reforming (Takeguchi et al., 2003; Youn et al., 2008a,b), and CO_2 reforming (Luna and Iriarte, 2008; Nandini et al., 2006). It must be noted that hydrogen production must be low in CO_2 emissions and other pollutants. Among all mentioned technologies, catalytic steam reforming of natural gas as a feasible process is widely used for hydrogen production, 80–85% of the world's total hydrogen production is provided by this method (Simpson and Lutz, 2007).

1.2. Steam reforming

Steam reforming technology is the most commercial method for synthesis gas (CO, H_2) production, the hydrogen cost is less than hydrogen produced by using renewable energy sources or from gasification of solid fossil fuel (Rostrup-Nielsen, 1993; Tugnoli et al., 2008). Steam reforming may involve several catalytic steps: desulfurization of the fuel, steam reforming of methane, a water gas shift reactor and purification of hydrogen using the PSA unit. This method is suitable for light hydrocarbons such as natural gas (mainly CH_4), naphtha, and liquefied petroleum gas (Ryden et al., 2006). Three main catalytic reactions involved in steam reformer reactor are steam reforming of methane (SRM) and the water–gas shift reaction.

$$CH_4 + H_2O \leftrightarrow CO + 3H_2, \qquad \Delta H^0_{298} = 206.3\ \text{kJ/mol} \tag{1}$$

$$CH_4 + 2H_2O \leftrightarrow CO_2 + 4H_2, \qquad \Delta H^0_{298} = 164.9\ \text{kJ/mol} \tag{2}$$

$$CO + H_2O \leftrightarrow CO_2 + H_2, \qquad \Delta H^0_{298} = -41.1\ \text{kJ/mol} \tag{3}$$

Conventional steam reformer consists of vertical tubes packed with Ni-based catalyst located inside the huge furnace. The required heat for endothermic reforming reaction is provided by direct combustion of fuel in the furnace. Therefore, the reformer tubes are under very high thermal stress (Brown, 2001). In order to solve this issue, the recuperative coupled reactor has been suggested in which an appropriate exothermic reaction is used as a heat source. Hunter and McGuire (1980) were pioneers in coupling endothermic and exothermic reactions without direct heat transfer. A review on the process intensification for methane steam reforming in a thermally coupled membrane separation technology was studied by Bhat and Sadhukhan (2009). Patel and Sunol (2007) suggested a thermally coupled membrane reactor that is composed of the three channels for methane steam reforming. A numerical model for natural gas, steam reforming and coupling with a furnace was developed by Ventura and Azevedo (2010). In an interesting idea, Ryden and Lyngfelt (2006) studied steam methane reforming coupled with a chemical looping combustion reactor in order to enhance H_2 production with CO_2 capture.

1.3. Catalytic oxidation of methane

Today, steam reforming and partial oxidation are the main technologies to produce synthesis gas from natural gas. However, there are two main operational issues in producing synthesis gas by using these methods; Firstly, obtaining the suited H_2/CO ratio and the second is reaching to high methane conversion and avoiding coke deposition (Jiang et al., 2007). For the characteristics of undesired H_2/CO ratio of steam methane reforming for production of methanol and Fischer–Tropsch Synthesis and also high energy cost due to its endothermic reaction, alternative routes have been investigated. In this way, many other methods have been studied, including: carbon dioxide reforming (Mark et al., 1997; Bradford and Vannice, 1999), the partial methane oxidation (Mallens et al., 1997; Nakagawa et al., 1998), combinations of these reaction routes (Choudhary et al., 1995, 1998; Ruckenstein and Hu, 1998) and Tri reforming (combination of CO_2 reforming, steam reforming, and partial oxidation) (Song, 2001). An effective option is to use catalytic oxidation of methane, which combines steam methane reforming and total combustion of methane in a single reactor. Four catalytic reactions of (1)–(4) are used to describe the oxidation of methane:

$$CH_4 + 2O_2 \leftrightarrow CO_2 + 2H_2O, \qquad \Delta H^0_{298} = -802.7\ \text{kJ/mol} \tag{4}$$

This reaction is exothermic, so that no need for an external heat supply and leads to significant reduction of the total costs. In addition, the heat of reaction can be a source of energy supply for one or two suitable endothermic reactions like steam reforming and propane dehydrogenation in a thermally coupled reactor.

1.4. Dehydrogenation of propane

In today's scenario, due to rapidly growing demand of alkenes, industrial procedure of corresponding alkanes dehydrogenation has received much attention. Alkenes, especially ethylene and propylene, are indispensable raw materials for numerous petrochemical products (Thapliyal and Deo, 2003). Propylene has wide application as the major feedstock for the production of diverse products, ranging from solvents to plastics like (Sahebdelfar et al., 2012; Budavari, 1996):

- Petrochemicals such as plastic polypropylene, acrolein and acrylic acid.
- Films, packaging, caps and closures.
- Isopropanol (Propan-2-ol), acrylonitrile, propylene oxide (epoxy propane) and epichlorohydrin.

Moreover, the propylene market reached the average growth rate of 5–6% per year (Tullo, 2003).

Propene is basically produced from fossil fuels, petroleum and natural gas via steam cracking and direct dehydrogenation (Warren and Oyama, 1996; Vitry et al., 2004). However, propane dehydrogenation is the economical and shortest route to propylene (Nawaz and Wei, 2011). The dehydrogenation reaction is a highly endothermic and equilibrium controlled; therefore, acceptable equilibrium conversion and reaction rate achieved with higher temperatures and lower pressure (Chin et al., 2011).

1.5. Thermally double coupled reactors

Recently, coupling exothermic and endothermic reactions are more interested in order to improve the thermal efficiency of the process and consequently enhances the production. This type of reactors aims to use energy released by exothermic reaction for proceeding endothermic reaction. In general, the coupled reactors exist into three main classes: direct coupling, recuperative coupling and finally regenerative coupling. At present, recuperative coupling has attracted the most attention of many researchers (Song et al., 2003). Coupling one endothermic and one endothermic reaction are more usual in this field. A double integrated reactor for dimethyl ether synthesis and H_2 production from the cyclohexane dehydrogenation has been suggested and mathematical model by Vakili et al. (2011). Rahimpour et al. (2011) also studied the methanol synthesis and the dehydrogenation of cyclohexane to benzene

in a thermally coupled membrane reactor with the aim of simultaneous methanol and hydrogen production. In 2010, Iranshahi et al. (2010) investigated an integrated process for the naphtha reforming process and the hydrogenation of nitrobenzene to aniline.

For the first time, economical thermally double coupled reactor in which two exothermic reactions are coupled with one endothermic reaction has been studied by Rahimpour et al. (2013a,b,c). Recently, the simultaneous production of methanol, hydrogen and gasoline in a thermally double coupled reactor has been investigated by Samimi et al. (2013). Also, Farniaei et al. (2013) have inserted dual membrane in the thermally double coupled reactor. In this study, double coupled dual membrane reactor has been used for simultaneous production of methanol, hydrogen and DME.

1.6. Literature review

Many efforts have been made for improvement of steam methane reforming. Arab Aboosadi et al. (2011b) have considered a novel integrated thermally coupled configuration for methane steam reforming. In their simulated reactor, hydrogenation of nitrobenzene to aniline in the exothermic side is used as a heat source for an endothermic reaction of steam methane reforming. The exothermic reaction takes place in the shell side and endothermic reaction occurs in the tube side. Moreover, Arab Aboosadi et al. (2011a) simulated and optimized tri-reformer (TRM) reactor for producing synthesis gas using differential evolution (DE) method. In TRM process, steam reforming, CO_2 reforming and partial oxidation of methane occurred in a single reactor. Finally, methane steam reforming and hydrogenation of nitrobenzene in hydrogen perm-selective membrane thermally coupled reactor has been optimized using differential evolution (DE) method by Rahimpour et al. (2013a). Recently, Rahimpour et al. (2013b) have simulated methane steam reforming technology coupled with fluidized bed chemical looping combustion using Fe-based as an oxygen carrier. From previous studies, it is found that there is no modeling information available in the literature about using oxidation of methane as a heat source for steam methane reforming in order to increase H_2 production. Therefore, it was decided to study on the mentioned system.

1.7. Objectives

The main goal of this study is an enhancement of synthesis gas production via steam reforming and oxidation of methane theoretically in a thermally double coupled steam reformer (TDCSR) in which propylene and hydrogen are also produced as additional valuable products. Two endothermic reactions of steam reforming and dehydrogenation of propane are coupled with exothermic reaction of oxidation of methane. The motivation is to combine the energy efficient concept of coupling one exothermic with two endothermic reactions, enhancement of synthesis gas production, propylene and hydrogen production and also producing two different H_2/CO ratio streams of syngas. A steady state 1-D homogeneous model of the thermally double coupled multitubular reactor is used to estimate the performance of the proposed reactor. Ultimately, the simulation results of the TDCSR were compared with the ones in conventional steam methane reforming.

2. Process description

2.1. Conventional steam reformer (CSR)

Fig. 1 represents the schematic diagram of a conventional Lurgi steam methane reformer to produce syngas for methanol synthesis process. This reactor has vertical tubes which are located inside a huge fired furnace. Natural gas is mixed with steam and entered to the steam reformer tubes as feed. Vertical tubes are packed with Ni-based catalyst and the generated heat related to natural gas combustion in burners of furnace transfers to reformer tubes (Methanol documents of Lurgi in Assaluyeh-Iran). Table 1 shows the specification of reactor and operating conditions of the CSR.

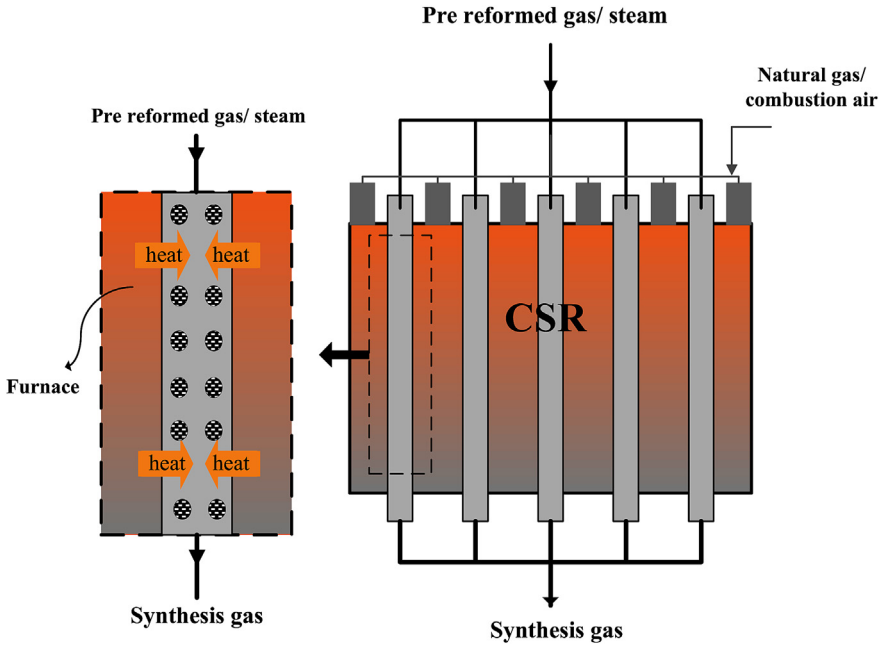

Fig. 1. A schematic diagram of conventional steam reformer (CSR).

Table 1
Characteristics and operating conditions of conventional steam reformer (CSR).

Parameter	Value
Tube side	
Feed composition (%mole)	
CH_4	32.59
H_2O	58.26
H_2	5.89
CO	0.02
CO_2	1.72
N_2	1.52
Inlet temperature (°C)	520
Inlet pressure (bar a)	40
Total feed gas flow (kmol/h)	9129.6
Number of tubes (in 4 rows)	184
Inside diameter (mm)	125
Heated length (m)	12
Catalyst volume filled in (total) (m^3)	27.8
Design pressure (bar g)	41
Design temperature (°C)	790
Catalyst shape	10-HOLE rings
Particle size (mm)	19 × 16
Void fraction	0.4
Heat load on tube (100% design case) (kcal/m^2 h) (based on tube ID)	68,730
Reformer duty (100% design case) (GJ/h) net	248.2
Shell side	
Combustion air	
Temperature (°C)	330
Pressure (bar a)	1
Flow rate (s m^3/h)	114,313
Feed gas (fuel)	
Temperature (°C)	34
Pressure (bar a)	3
Flow rate (s m^3/h)	29,608

2.2. Thermally double coupled steam reformer (TDCSR)

A conceptual schematic diagram of TDCSR is shown in Fig. 2. This innovative configuration has three concentric tubes in which exothermic reaction of methane oxidation takes place co-currently in the middle tube. Steam reforming of natural gas and dehydrogenation of propane are occurring in the inner and outer tubes, respectively as two endothermic sides. Two streams of syngas, propylene and hydrogen exit from bottom of the reactor. The specific properties and operational conditions of TDCSR are tabulated in Tables 2 and 3. Table 1 (excluding data on the shell side) is also used for endothermic side of thermally double coupled steam reformer.

3. Reaction scheme and kinetics

3.1. Steam methane reforming (inner endothermic side)

Three main reactions occurred in steam reformer are steam reforming of methane and the water–gas shift reaction (Equations (1)–(3)). The reaction rates of CSR reactions proposed as follows (Xu et al., 2002; Xu and Froment, 1989):

$$R_1 = \frac{k_1}{P_{H_2}^{2.5}}\left(P_{CH_4}P_{H_2O} - \frac{P_{H_2}^3 P_{CO}}{K_I}\right)\times\frac{1}{\varphi^2} \tag{5}$$

$$R_2 = \frac{k_2}{P_{H_2}^{3.5}}\left(P_{CH_4}P_{H_2O}^2 - \frac{P_{H_2}^4 P_{CO_2}}{K_{II}}\right)\times\frac{1}{\varphi^2} \tag{6}$$

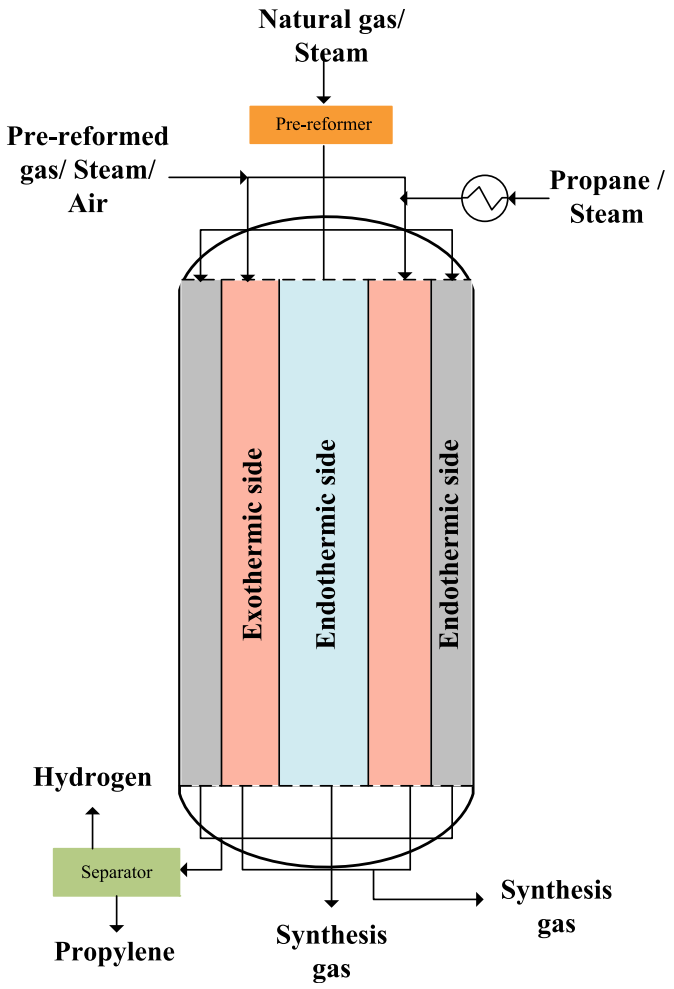

Fig. 2. A scheme of novel thermally double coupled steam reformer (TDCSR) configuration.

$$R_3 = \frac{k_3}{P_{H_2}}\left(P_{CO}P_{H_2O} - \frac{P_{H_2}P_{CO}}{K_{III}}\right)\times\frac{1}{\varphi^2} \tag{7}$$

$$\varphi = 1 + K_{CO}P_{CO} + K_{H_2}P_{H_2} + K_{CH_4}P_{CH_4} + K_{H_2O}\frac{P_{H_2O}}{P_{H_2}} \tag{8}$$

The reaction equilibrium constants and Arrhenius kinetic parameters are listed in Table 4. Table 5 shows the Van't Hoff parameters for species adsorption.

3.2. Catalytic oxidation of methane (exothermic side)

As said before, four catalytic reactions of (1)–(4) are selected to describe the oxidation of methane. The reaction rate of methane combustion (ex. 4) is as follows:

$$R_4 = \frac{k_{4a}p_{CH_4}p_{O_2}}{\left(1 + K_{CH_4}^C p_{CH_4} + K_{O_2}^C p_{O_2}\right)} + \frac{k_{4b}p_{CH_4}p_{O_2}}{\left(1 + K_{CH_4}^C p_{CH_4} + K_{O_2}^C p_{O_2}\right)} \tag{9}$$

Tables 4 and 5 also include additional information for calculating this rate of reaction.

Table 2
The operating conditions for catalytic oxidation of methane (exothermic side) and propane dehydrogenation side.

Parameters	Values
Catalytic oxidation of methane	
Catalyst density (kg/m^3)	2250
Bed void fraction	0.4
Inlet temperature (K)	860
Inlet pressure (bar)	20
Total molar flow rate (mol/s)	7.5
Feed composition (% mole)	
CH_4	26.81
H_2O	48.40
H_2	2.03
CO	0.01
CO_2	2.24
O_2	20.5
N_2	0.01
Propane dehydrogenation	
Bed void fraction	0.4
Inlet temperature (K)	800
Inlet pressure (bar)	1
Total molar flow rate (mol/s)	0.5
Feed composition (% mole)	
C_3H_8	62
H_2	38
C_3H_6	0
CH_4	0
C_2H_4	0

Table 3
Specifications of thermally double coupled steam reformer (TDCSR).

Parameters	Values
Inner tube or steam reforming side diameter (m)	125×10^{-3}
Middle tube or exothermic side diameter (m)	165×10^{-3}
Outer tube or propane dehydrogenation side diameter (m)	185×10^{-3}
Length of the reactor (m)	12

3.3. Dehydrogenation of propane (outer exothermic side)

The main reaction on the outer side is dehydrogenation of propane. Moreover, two other reactions of propane cracking and hydrogenolysis reaction are also occurring. All of the following reactions are taken into consideration for dehydrogenation of propane in the outer exothermic side:

$$C_3H_8 \leftrightarrow C_3H_6 + H_2, \quad \Delta H^0_{298} = +129\ \text{kJ/mol} \tag{10}$$

$$C_3H_8 \leftrightarrow C_2H_4 + CH_4, \quad \Delta H^0_{298} = +79.4\ \text{kJ/mol} \tag{11}$$

$$C_3H_8 + H_2 \leftrightarrow C_2H_6 + CH_4, \quad \Delta H^0_{298} = -63.4\ \text{kJ/mol} \tag{12}$$

Table 5
Van't Hoff parameters for components adsorption.

	K_{oi} (bar^{-1})	ΔH (J/mol)	K^C_{oi} (bar^{-1})	ΔH^C_i (J/mol)
CH_4	6.65×10^{-4}	−38,280		
CO	8.23×10^{-5}	−70,650		
H_2	6.12×10^{-9}	−82,900		
H_2O	1.77×10^{-5} bar	88,680		
CH_4 (combustion)			1.26×10^{-1}	−27,300
O_2 (combustion)			7.78×10^{-7}	−92,800

$K_i = K_{oi} \times \exp\left(-\frac{\Delta H}{RT}\right)$

$K^C_i = K^C_{oi} \times \exp\left(-\frac{\Delta H^C_i}{RT}\right)$

The following expressions are the correspondent rate equations for above reactions (Chin et al., 2011):

$$r_1 = a \times k_1 \left(1 - \frac{P_{C_3H_6} \times P_{H_2}}{P_{C_3H_8} \times K_{eq}}\right) \frac{P_{C_3H_8}}{P^{.5}_{H_2} + K_{C_3H_6} \times P_{C_3H_6}} \tag{13}$$

$$r_2 = k_2 P_{C_3H_8}, \quad k_2 = 33 \exp\left(\frac{-137,000}{RT}\right) \tag{14}$$

$$r_3 = k_3 P_{C_3H_8} P_{H_2}, \quad k_3 = 2.4 \times 10^{-9} \exp\left(\frac{-137,000}{R}\left(\frac{1}{T} - \frac{1}{793.15}\right)\right) \tag{15}$$

where

$$K_{eq} = 8.49 \times 10^8 \exp(-118,707/(RT))\ (\text{kPa}),$$
$$k_1 = 0.3874 \exp(-2950/T)\ \left(\text{kmol}\Big/\left(\text{s m}^3\ \text{kPa}^{.5}\right)\right), \tag{16}$$
$$K_{C_3H_6} = 3.4785 \times 10^{-8} \exp(17200/T)\ (\text{kPa})^{-0.5}$$

4. Mathematical model

Fig. 3 shows a schematic diagram for co-current mode of the thermally double coupled steam reformer reactor configuration. One-dimensional homogeneous model, including a set of coupled mass and energy balances is taken into consideration. The hypotheses considered in the model of the three sides are summarized as follows:

- Steady state condition.
- Gas phase is considered as an ideal.
- Plug flow pattern is assumed.
- Bed porosity in axial and radial direction is constant.
- Heat loss is neglected.

Table 4
Reaction equilibrium constants and Arrhenius kinetic parameters.

Reaction, j	Equilibrium constant, K_j	k_{oj} (mol/(kgcat s))	E_j (J/mol)
1	$K_I = \exp\left(\frac{-26830}{T} + 30.114\right)$ (bar^2)	1.17×10^{15} bar$^{0.5}$	240,100
2	$K_{II} = K \ldots K$ (bar^2)	2.83×10^{14} bar$^{0.5}$	243,900
3	$K_{III} = \exp\left(\frac{4400}{T} - 4.036\right)$	5.43×10^{-5} bar^{-1}	67,130
4		8.11×10^{-5} bar^{-2}	86,000
		8.62×10^{-5} bar^{-2}	86,000

$k_j = k_{oj} \times \exp\left(-\frac{E_j}{RT}\right)$

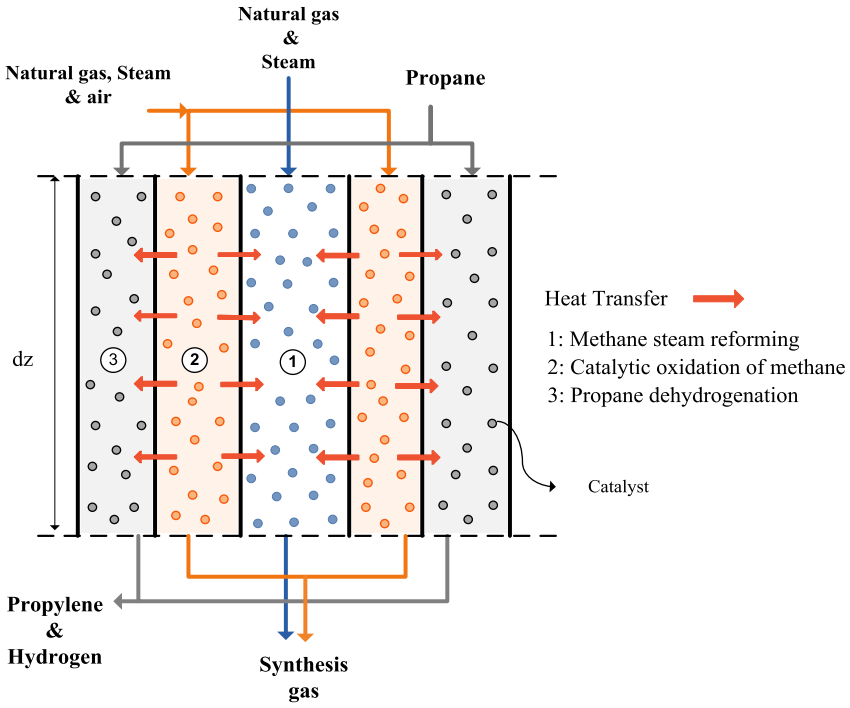

Fig. 3. A differential element along the length of TDCSR.

- Axial diffusion of mass and heat is ignored.

Based on the above assumptions and considering the element with length Δz along the axial direction, the differential equations describing mole and energy transfers are obtained.

The mass and energy balances for fluid and solid phases are listed in Table 6.

Where T is temperature of each side and η is effectiveness factor defined as the ratio of the reaction rate observed in the real rate of reaction. The effectiveness factors of each reaction of steam reforming side are: $\eta_1 = 0.07$, $\eta_2 = 0.06$, $\eta_3 = 0.7$ (De Groote and Froment, 1996).

4.1. Auxiliary correlations

In order to complete the mentioned simulation equations, auxiliary correlations containing physical properties of components, mass and heat transfer coefficients should be added, see Table 7.

5. Numerical solution

A governing equation of this model consists of a set of differential algebraic equations including mass balances for all sides with given boundary conditions incorporate with the reaction rates as well as basic assumptions. In order to solve the set of equations, backward finite difference approximation was used. The reactor length is then divided into 100 separate sections and the Gauss–Newton method in MATLAB programming environment was used to solve the non-linear algebraic equations in each section.

6. Simulation and results

Model validation was carried out by comparing the simulated results of the steam reforming side of thermally double coupled steam reformer (TDCSR) with the observed experimental data of the industrial tubular fixed bed steam reformer reactor which is shown in Fig. 4. According to this figure, this simulation result is in good agreement with experimental data.

Table 6
Mass and energy balances equations and boundary conditions.

Definitions	Equations	
Mass balance for exothermic and endothermic sides	$-\frac{dF^g_{i,k}}{dz} + \rho_b A_{C_k}\left(\sum_{j=1}^{m} r_j \eta_j \upsilon_{ij}\right) = 0$	(17)
Energy balance for exothermic side	$-\frac{d\left(C^g_{Pk} F^g_{i,k}\left(T^g_k - T_{ref}\right)\right)}{dz} - U_{k-2}\pi D_k\left(T^g_k - T^g_2\right) - \rho_b A_{C_j}\alpha\left(\sum \Delta H_{f,j} r_j \eta_j\right) = 0$	(18)
Energy balance for endothermic side	$-\frac{d\left(C^g_{P2} F^g_{i,2}\left(T^g_2 - T_{ref}\right)\right)}{dz} + U_{1-2}\pi D_1\left(T^g_1 - T^g_2\right) + U_{3-2}\pi D_3\left(T^g_3 - T^g_2\right) - \rho_b A_{C_j}\alpha\left(\sum \Delta H_{f,j} r_j \eta_j\right) = 0$	(19)
Boundary conditions	$z = 0,\ F_i = F_{i0},\ T = T_0,\ P = P_0$	(20)

Table 7
Auxiliary correlations.

Definitions	Equations
Heat capacity of components	$C_P = C_1 + C_2\left[\frac{(C_3/T)}{\sinh(C_3/T)}\right]^2 + C_4\left[\frac{(C_5/T)}{\cosh(C_5/T)}\right]^2$
Heat capacity of gas mixture	Based on local compositions
Viscosity of components	$\mu = \frac{C_1 T^{C_2}}{1+(C_3/T)+(C_4/T^2)}$
Viscosity of gas mixture	$\mu_m = \frac{\sum y_i \cdot \mu_i \cdot M_{W,i}^{S}}{\sum y_i \cdot M_{W,i}^{S}}$
Overall heat transfer coefficient	$\frac{1}{U} = \frac{1}{h_i} + \frac{A_i \ln(D_o/D_i)}{2\pi L K_w} + \frac{A_i}{A_o}\frac{1}{h_o}$
Heat transfer coefficient between gas phase and reactor wall	$\frac{h}{C_p \rho \mu}\left(\frac{C_p \mu}{K}\right)^{2/3} = \frac{0.458}{\varepsilon_B}\left(\frac{\rho u d_p}{\mu}\right)^{-0.407}$
Ergun equation	$\frac{dp}{dz} = 150\frac{(1-\varepsilon)^2 \mu Q}{\varepsilon^3 dp^2 A_c} + 1.75\frac{(1-\varepsilon)\rho Q^2}{\varepsilon^3 dp A_c^2}$

6.1. Thermal behavior

Fig. 5(a) shows the axial temperature profiles in conventional steam reformer reactor (CSR) as well as the inner endothermic side of thermally double coupled steam reformer (TDCSR). As seen, the temperature profile of CSR is linear while it has a curvy profile in the TDCSR. Although the initial temperature of both configurations is the same, the temperature profile of TDCSR is higher than that of CSR as a result of the positive effect of coupling concept which improves the overall heat transfer coefficient. Since the rates of endothermic reactions increase as temperature increases, syngas production is improved in TDCSR. Fig. 5(b) represents the thermal behavior of all sides of TDCSR. In order to make a driving force for heat transfer from exothermic side to endothermic side, the temperature of endothermic side must be always lower than that of exothermic side. In general, the highest temperature in thermally couple reactors is related to exothermic side where heat generation occurs. Although steam reforming is an endothermic process, its temperature is increased along the reactor; it happens because the amount of heat generated in the exothermic side is much higher than the consumed heat in the endothermic side (see Fig. 6(a)). The most heat transfer takes place in the first half of the reactor because of high temperature difference between both endothermic sides and exothermic side. At the end of the reactor, temperature of each three sides reaches to an equal value since the heat transferred from exothermic side to both endothermic sides, becomes zero.

Fig. 6(a) shows the consumed, heat and transferred heat in the steam methane reforming (inner endothermic side) of TDCSR. The consumed, heat of inner side is lower than the transferred heat from the exothermic side so the temperature increases along the reactor length in this side. At the end of the reactor, both heats have nearly the same profile causes constant temperature. Part of generating heat from the oxidation side is used for driving two endothermic reactions and the rest is used to heat the reaction mixtures in three sides of TDCSR. In the length of 0.12 m, there is a maximum in the consumer and transferred heat, which means that the maximum reaction rating takes place on this part. Fig. 6(b) demonstrates the consumption and transferred heat of outer endothermic side in which propane dehydrogenation occurs. In the first 0.12 m of the thermally double coupled steam reformer reactor, exothermic reaction of hydrogenolysis is the predominant reaction in the dehydrogenation side so the consumed heat decreases in this part. At the length of 1.68 m, the consumed, heat and transferred heat have become the same. After that, the consumed, heat profile became higher than transferred heat results in decreasing the temperature as seen in Fig. 5(b).

6.2. Molar behavior

6.2.1. Steam reforming of methane (inner endothermic side)

Fig. 7(a)–(e) presents the comparison of mole fraction of components in inner endothermic side (steam methane reforming) of

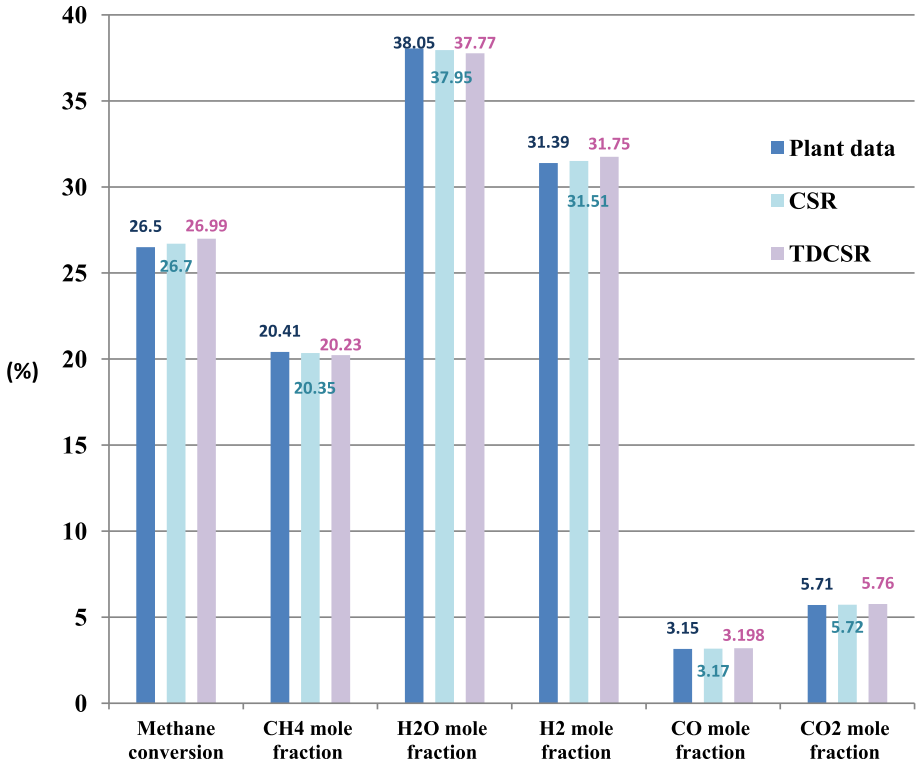

Fig. 4. A comparison between the results of simulation and plant data.

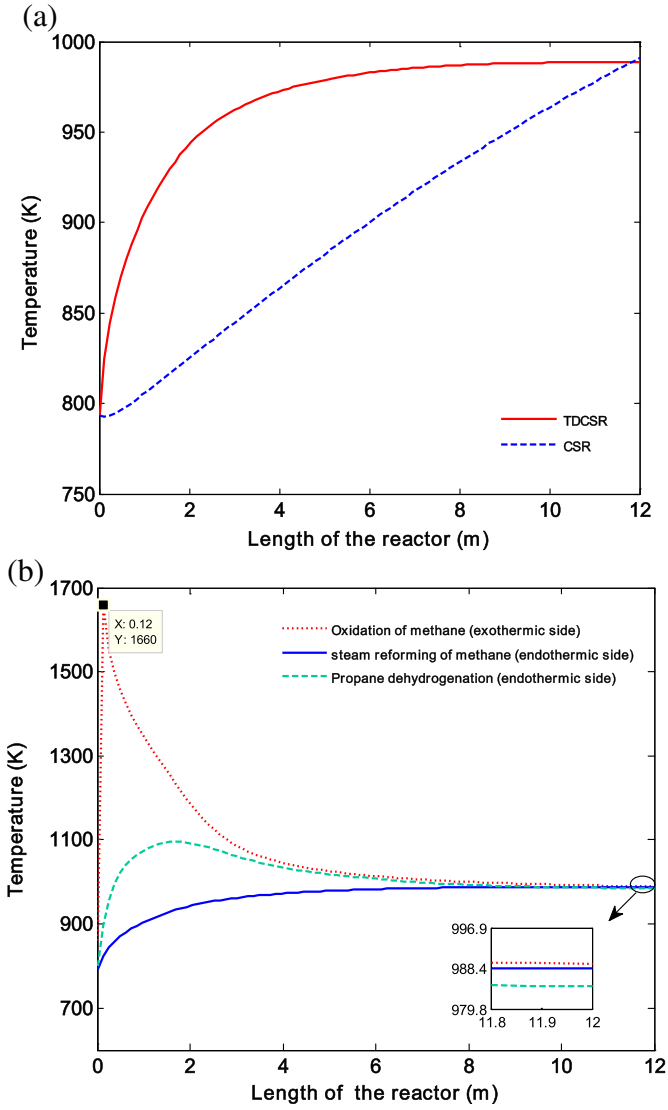

Fig. 5. (a) A comparison between temperatures in the CSR and methane steam reforming side of TDCSR, (b) Temperature profiles of methane steam reforming, methane catalytic oxidation and propane dehydrogenation sides along the reactor.

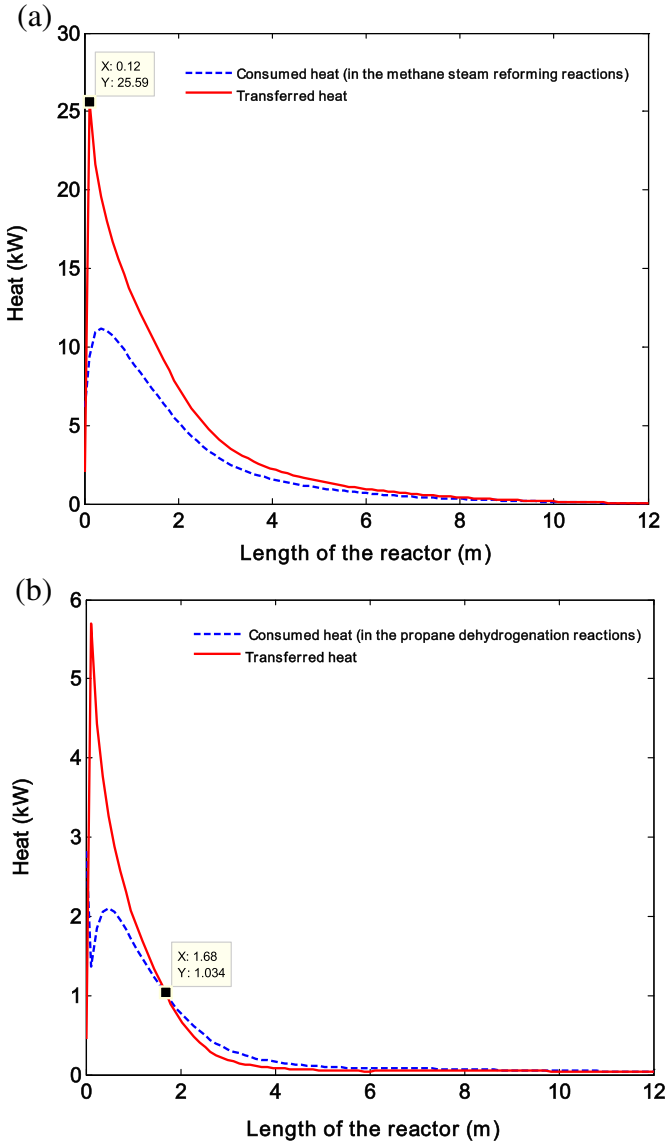

Fig. 6. (a) Transferred and consumed heats related to the steam reforming and (b) propane dehydrogenation sides along the length of TDCSR.

TDCSR and CSR. Fig. 7(a) and (b) illustrates the mole fraction of hydrogen and carbon monoxide (CO) along the reactor at steady state. Hydrogen and CO are the most desirable products of steam reforming and fortunately their mole fractions increase along the reactor in the double coupled configuration in comparison with CSR, because the thermal effect of coupled reactor provides a good condition for heat transfer and consequently more production. At the end of the reactor, both reactors reach to each others. The CH_4 mole fraction is depicted in Fig. 7(c). As can be seen, the consumption rate of CH_4 as a main reactant in steam methane reforming process increases in coupled configuration. The difference between CH_4 mole fraction profiles in CSR and TDCSR is owing to the temperature increase in endothermic side which causes the increase in reaction rate and CH_4 consumption (see Fig. 5(a)). CO_2 and H_2O mole fraction as an undesired product in TDCSR is compared with the one in CSR in Fig. 7(d) and (e), respectively. Along the reactor length, the water mole fraction in TDCSR is lower than the one in the CSR configuration, but at the end of the reactor it becomes the same as conventional reactor. After the reactor length of 8 m, all mole factions have become constant; it shows the economical feature of the thermally double coupled steam reformer which have the same production in a shorter length than conventional reactor (12 m).

6.2.2. *Oxidation of methane (exothermic side)*

Fig. 8 demonstrates the mole fractions of components in exothermic side of TDCSR in which oxidation of methane occurred. As the reaction scheme shows, the mole fraction of CH_4 and O_2, as reactants, decreases along the middle tube; after proceeding 0.12 m of the reactor, mole fraction of O_2 reaches to zero as a result of predominating the reaction of methane combustion in this part. As seen, the mole fractions of H_2 and CO_2 increase as the main product of steam reforming and water gas shift reactions. From 0.12 m to 3.5 m, steam reforming reactions proceed more than total combustion of methane owing to the high temperature of exothermic side; so the mole fraction of hydrogen and CO_2 increase. After 3.5 m, the temperature of exothermic side decreases and consequent the reactions of reforming shifts toward reactant side (left side) and as a result, the mole fractions of methane and water increase. The

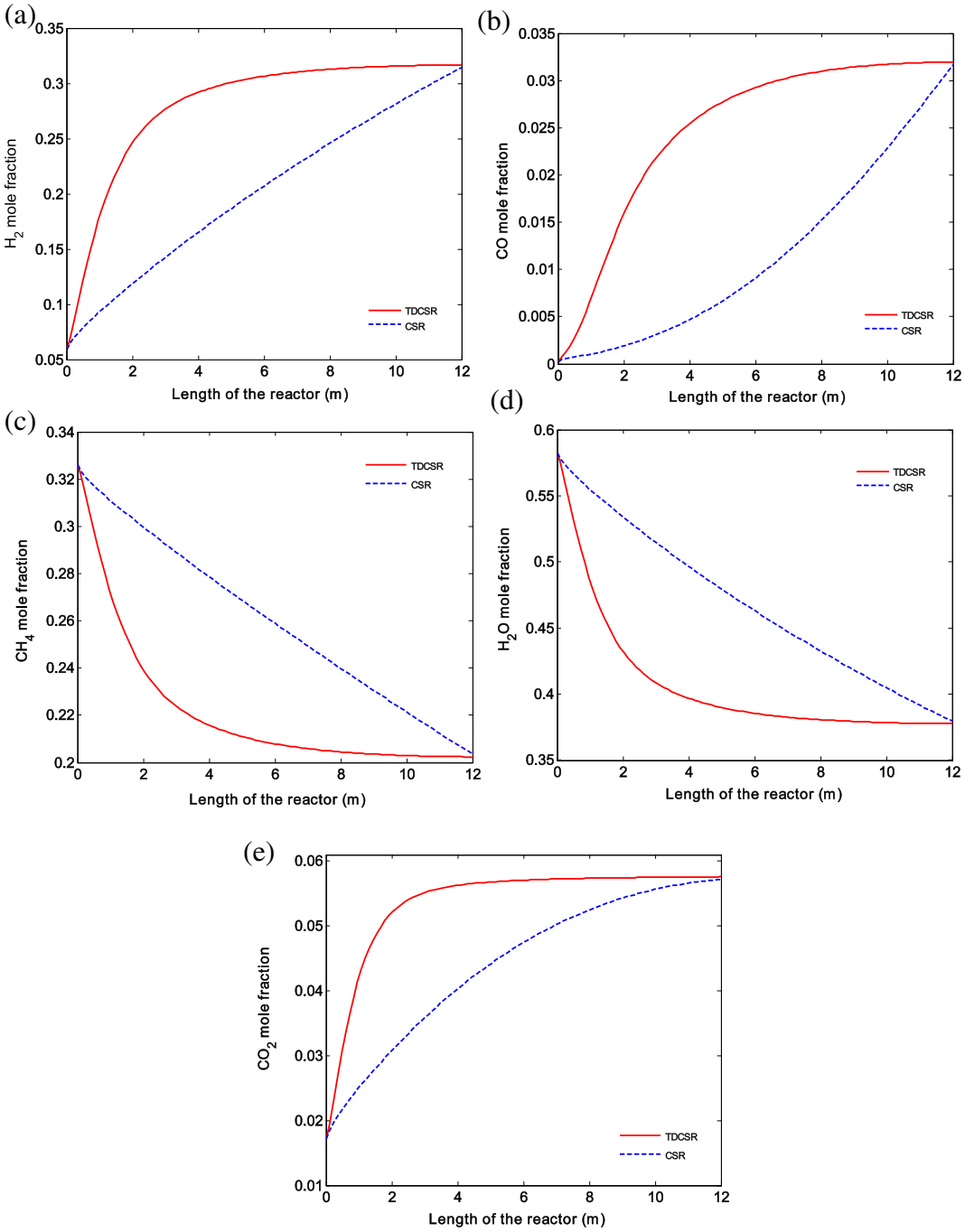

Fig. 7. A comparison of (a) H_2 mole fractions, (b) CO mole fractions, (c) CH_4 mole fractions, (d) H_2O mole fractions, (e) CO_2 mole fractions.

mole fraction of CO of the reactor entrance increases and then decreases as consuming in the water gas shift reaction.

6.2.3. Dehydrogenation of propane (outer endothermic side)

Fig. 9(a) and (b) illustrates the mole fraction of the components of dehydrogenation side. Comparing Fig. 7(a) with Fig. 7(b) shows that the mole fraction of C_3H_6 and H_2 are much higher than C_2H_4, CH_4 and C_2H_6, for the dehydrogenation of propane is the predominant reaction on this side and the rate of propane cracking and propane hydrogenolysis are low. The mole fractions of propylene and hydrogen reach to 0.358 and 0.6 at the end of the reactor.

6.3. Yield and conversion changes

In order to calculate CH_4 and propane conversion and hydrogen yield, the following formula is used:

$$\text{Methane conversion} = 100 \times \frac{F_{CH_4,in} - F_{CH_4,out}}{F_{CH_4,in}} \tag{21}$$

$$\text{Propane conversion} = \frac{F_{C_3H_8,out} - F_{C_3H_8,in}}{F_{C_3H_8,in}} \tag{22}$$

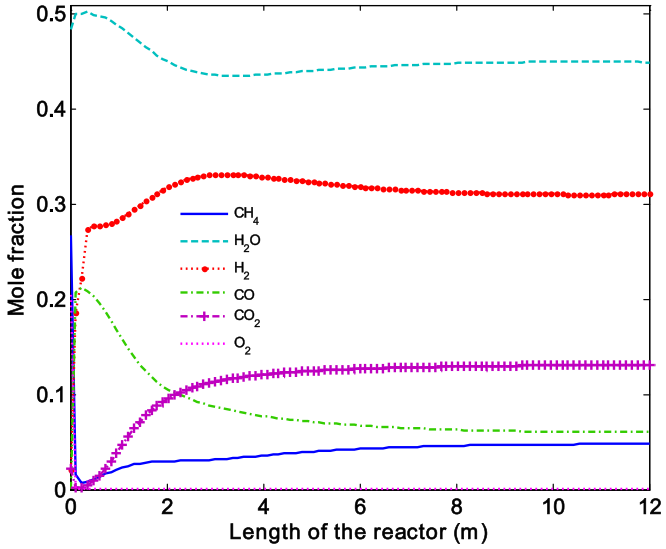

Fig. 8. Mole fractions of components in the methane catalytic oxidation side along the length of TDCSR.

$$\text{Hydrogen recovery yield (in the inner tube)} = \frac{F_{H_2,\text{out}} - F_{H_2,\text{in}}}{F} \tag{23}$$

$$\text{Hydrogen recovery yield (in outer tube)} = \frac{F_{H_2,\text{out}} - F_{H_2,\text{in}}}{F_{C_3H_8,\text{in}}} \tag{24}$$

Fig. 10 shows the conversion of methane in the CSR and TDCSR. According to this figure, conversion of methane in the TDCSR has a higher profile than CSR along the reactor. However, at the end of the reactor two profiles reach to a single point of 26%. Fig. 11(a) presents the effect of variation of inlet temperature on the output CH_4 conversion and H_2 yield of methane catalytic oxidation side. It can be understood from this figure that methane conversion and hydrogen yield increase as inlet temperature increase from 800 to 1100 K. Since the rates of endothermic reactions increase as temperature increases, 5.6 and 1.15% enhancement in the methane conversion and hydrogen yield are seen, respectively. Fig. 11(b) represents the propane conversion and hydrogen recovery yield in the outer endothermic side, simultaneously. At the first 2 m of the reactor, propane conversion jump occurs because the temperature of dehydrogenation increased with this length of the reactor (see Fig. 5(b)). After that, the conversion of propane slightly increases. Finally, the conversion of propane and hydrogen recovery yield reach to 91.35 and 89.47%.

6.4. The effect of inlet temperature on production

Fig. 12(a) and (b) shows the methane conversion and hydrogen yield as a function of inlet temperature and length in the methane steam reforming side. Both parameters (CH_4 conversion and H_2 yield) increase along the reactor length with increasing inlet temperature of steam reforming side due to increasing production of endothermic reactions with increasing temperature. As seen, methane conversion increased from 26.99 to 27.57% when the temperature increased from 793 to 840 K.

The effect of inlet temperature of propane dehydrogenation side (outer endothermic side) on the C_3H_8 conversion and H_2 yield is shown in Fig. 13(a) and (b), respectively. Temperature increasing of 200 K reaches the propane conversion to 90.13%. In addition,

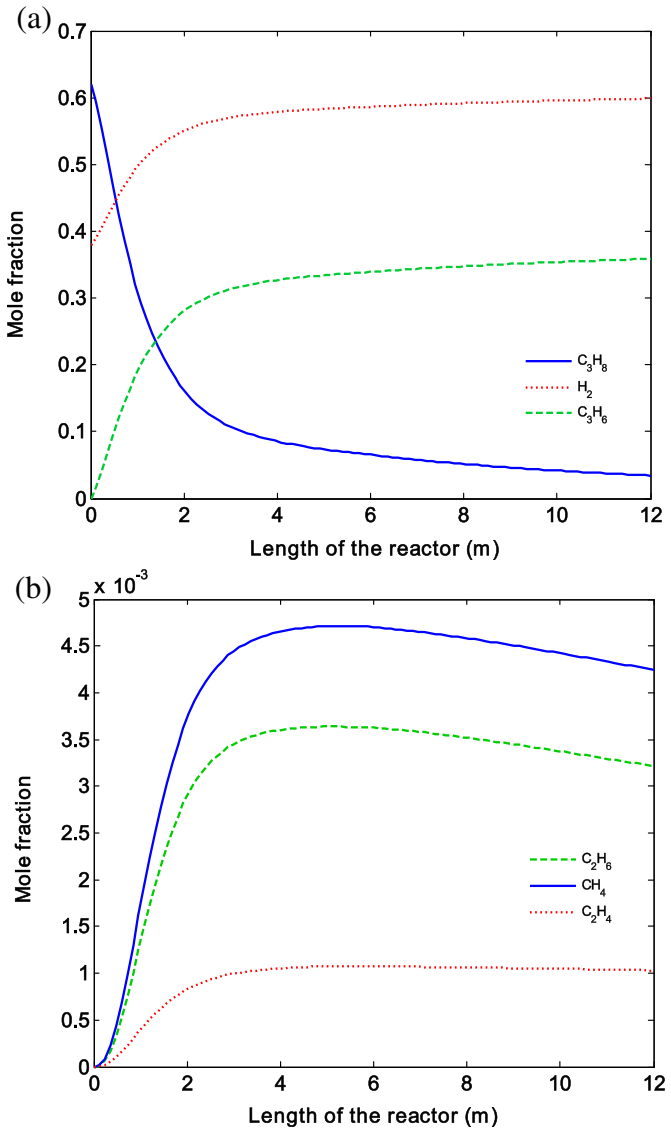

Fig. 9. (a) Mole fractions of C_3H_8, H_2 and C_3H_6 components and (b) mole fractions of C_2H_6, CH_4 and C_2H_4 components in the propane dehydrogenation side along the length of the TDCSR.

the hydrogen yield of dehydrogenation side increased with increasing temperature and reaches to 87.49% at the end of the reactor.

7. Conclusion

This work focuses on the simultaneous production of synthesis gas, hydrogen and propylene in a thermally double coupled steam reformer (TDCSR). In this novel configuration, the exothermic reaction of methane oxidation has coupled with two endothermic reactions; steam reforming of methane and dehydrogenation of propane to get a heat transfer better. Thermally coupled steam reformer consists of three concentric tubes; the inner, middle and outer sides are used for steam methane reforming, methane oxidation and propane dehydrogenation, respectively. A steady state homogeneous catalytic reaction model is applied to analyze the performance of TDSCR for simultaneous production of synthesis gas, hydrogen and propylene. The simulation results of

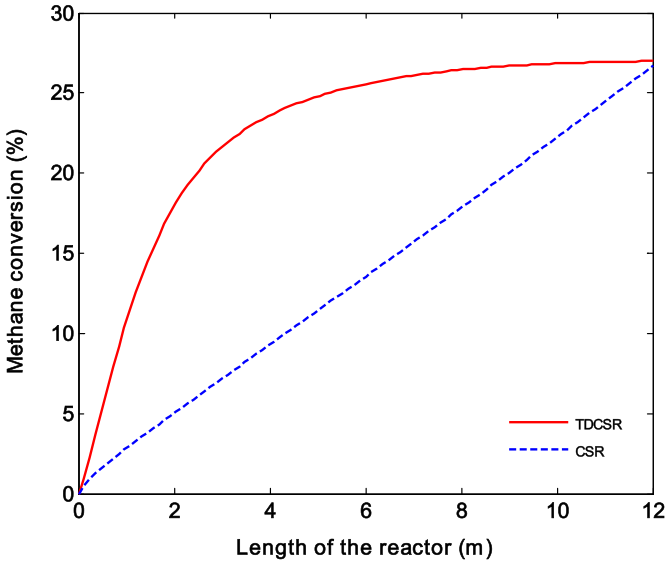

Fig. 10. Methane conversions in the CSR and methane steam reforming side of TDCSR.

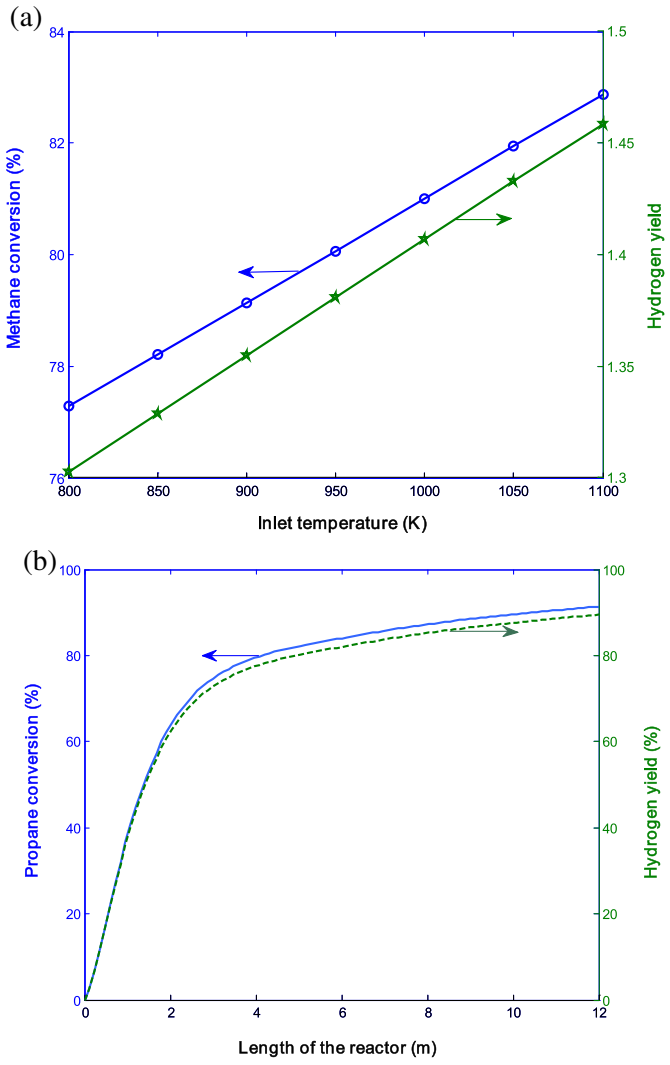

Fig. 11. (a) The effect of variation of inlet temperature on the output CH_4 conversion and H_2 yield of methane catalytic oxidation side, (b) C_3H_8 conversion and H_2 yield of propane dehydrogenation side along the length of the TDCSR.

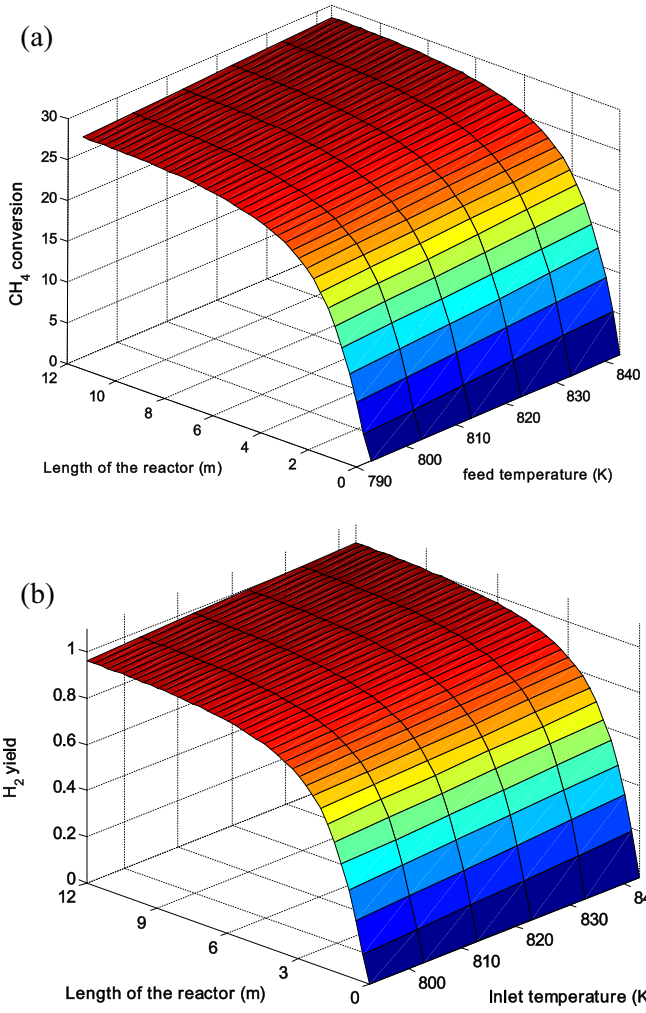

Fig. 12. (a) Methane conversion and (b) hydrogen yield as function of inlet temperature and length in the methane steam reforming side.

TDCSR have been compared with corresponding predictions for an industrial steam reformer operated at the same feed conditions. By this narrative configuration, not also the synthesis gas production increased, but also hydrogen, propylene and suitable syngas (with lower H_2/CO from the methane oxidation side) produce as additional valuable products. In addition, this thermally double coupled reactor reduces the capital and operating costs by reducing the reactor size and consumption of energy. The result demonstrates that thermally double coupled steam reformer is more economical and efficient than conventional reactor.

Nomenclature

A_a	cross section area of each tube (m^2)
av	specific surface area of catalyst pellet ($m^2\ m^{-3}$)
b	stochiometric factor for reaction in CLC
C^g	gas concentration ($mol\ m^{-3}$)
cp^g	specific heat of the gas at constant pressure ($J\ mol^{-1}$)
cp^s	heat capacity of oxygen carrier in CLC ($J\ kg^{-1}\ K^{-1}$)
D_i	inside diameter of steam reformer (m)
F_t	total flow rate per each reaction side ($mol\ s^{-1}$)
K_1	reaction rate constant for 1st rate equation of steam reforming ($mol\ kg^{-1}\ s^{-1}$)

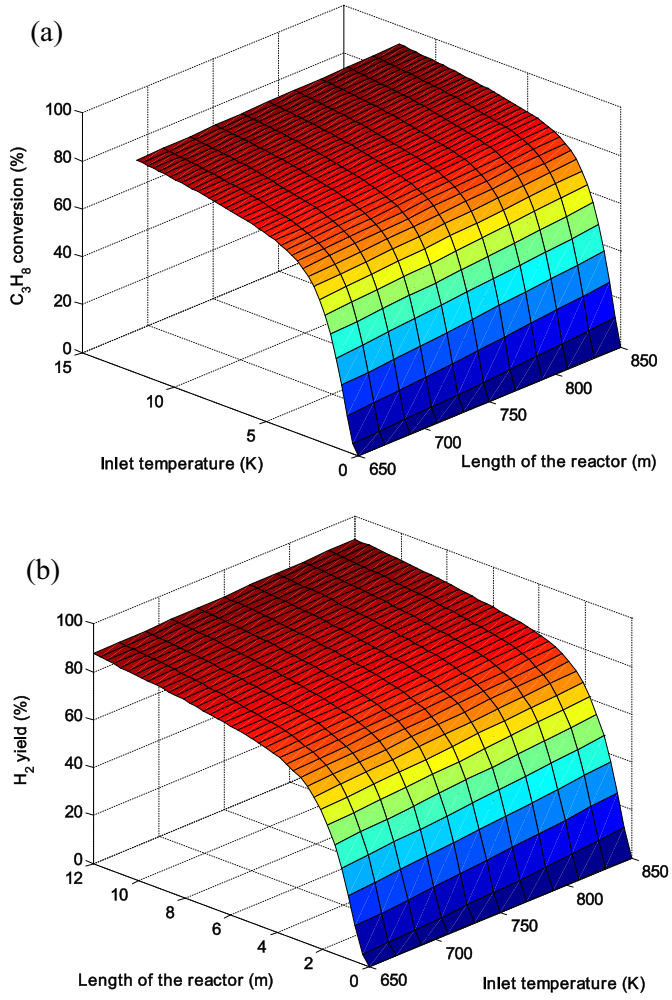

Fig. 13. (a) Propane conversion and (b) hydrogen yield as function of inlet temperature and length in the propane dehydrogenation side.

K_2	reaction rate constant for 2nd rate equation of steam reforming (mol kg^{-1} s^{-1})
K_3	reaction rate constant for 3rd rate equation of steam reforming (mol kg^{-1} s^{-1})
K_j	chemical reaction constant of j reaction (j = oxidation, reduction) (mol^{1-n} m^{3n-2} s^{-1})
N	number of components
n	reaction order
R_1	first rate of reaction for steam reforming of CH_4 (reaction (4)) (mol kg^{-1} s^{-1})
R_2	second rate of reaction for steam reforming of CH_4 (reaction (5)) (mol kg^{-1} s^{-1})
R_3	water gas shift reactor (reaction (6)) (mol kg^{-1} s^{-1})
r_1	rate of dehydrogenation of propane (kmol m^{-3} s^{-1})
r_2	rate of propane cracking reaction (kmol m^{-3} s^{-1})
r_3	rate of hydrogenolysis reaction (kmol m^{-3} s^{-1})
t	reaction time (s)
T	temperature (K)
U	overall heat transfer coefficient (W m^{-2} K^{-1})

Subscripts

0	inlet condition
i	chemical species
j	oxidation, reduction

Greek letters

ΔH_{fi}	enthalpy of formation of component (J mol^{-1})
ΔH_{RXn}	enthalpy of reaction (J mol^{-1})
ρ_b	density of catalyst bed (kg m^{-3})
η	effectiveness factor used for the intra particle transport limitation

References

Arab Aboosadi, Z., Jahanmiri, A.H., Rahimpour, M.R., 2011a. Optimization of tri-reformer reactor to produce synthesis gas for methanol production using differential evolution (DE) method. Appl. Energy 88, 2691–2701.

Arab Aboosadi, Z., Rahimpour, M.R., Jahanmiri, A., 2011b. A novel integrated thermally coupled configuration for methane-steam reforming and hydrogenation of nitrobenzene to aniline. Int. J. Hydrogen Energy 36, 2960–2968.

Bhat, S.A., Sadhukhan, J., 2009. Process intensification aspects for steam methane reforming: an overview. AIChE J. 55, 408–422.

Bradford, M.C.J., Vannice, M.A., 1999. CO_2 reforming of CH_4. Catal. Rev. Sci. Eng. 41, 1–42.

Brown, L.F., 2001. A comparative study of fuels for on-board hydrogen production for fuel-cell-powered automobiles. Int. J. Hydrogen Energy 26, 381–397.

8034. Propylene. In: Budavari, S. (Ed.), The Merck Index, 12th ed. Merck & Co., New Jersey, pp. 1348–1349.

Chin, S.Y., Radzi, S.N.R., Maharon, I.H., Shafawi, M.A., 2011. Kinetic model and simulation analysis for propane dehydrogenation in an industrial moving bed reactor. WASET 52, 183.

Choudhary, V.R., Rajput, A.M., Prabhakar, B., 1995. Energy efficient methane-to-syngas conversion with low H_2/CO ratio by simultaneous catalytic reactions of methane with carbon dioxide and oxygen. Catal. Lett. 32, 391–396.

Choudhary, V.R., Uphade, B.S., Mamman, A.S., 1998. Simultaneous steam and CO_2 reforming of methane to syngas over NiO/MgO/SA-5205 in presence and absence of oxygen. Appl. Catal. A 168, 33–46.

De Groote, A.M., Froment, G.F., 1996. Simulation of the catalytic partial oxidation of methane to synthesis gas. Appl. Catal. A 138, 245–264.

Farniaei, M., Abbasi, M., Rasoolzadeh, A., Rahimpour, M.R., 2013. Enhancement of methanol, DME and hydrogen production via employing hydrogen permselective membranes in a novel integrated thermally double-coupled two-membrane reactor. J. Nat. Gas Sci. Eng. 14, 158–173.

Gao, X.X., Huang, C.J., Zhang, N.W., Li, J.H., Weng, W.Z., Wan, H.L., 2008. Partial oxidation of methane to synthesis gas over Co/Ca/Al_2O_3 catalysts. Catal. Today 131, 211–218.

Heinzel, A., Vogel, B., Hubner, P., 2002. Reforming of natural gas–hydrogen generation for small scale stationary fuel cell systems. J. Power Sources 105 (2), 202–207.

Hunter, J.B., McGuire, G., 1980. Method and Apparatus for Catalytic Heat-exchange (US Patent 4 214 867).

Iranshahi, D., Bahmanpour, A.M., Pourazadi, E., Rahimpour, M.R., 2010. Mathematical modeling of a multi-stage naphtha reforming process using novel thermally coupled recuperative reactors to enhance aromatic production. Int. J. Hydrogen Energy 35 (20), 10984–10993.

Itoh, N., Watanabe, S., Kawasoe, K., Sato, T., Tsuji, T., 2008. A membrane reactor for hydrogen storage and transport system using cyclohexane–methylcyclohexane mixtures. Desalination 234, 261–269.

Jiang, H., Li, H., Xu, H., Zhang, Y., 2007. Preparation of Ni/$Mg_xTi_{1-x}O$ catalysts and investigation on their stability in tri-reforming of methane. Fuel Process. Technol. 88, 988–995.

Kim, P., Kim, Y., Kim, H., Song, I.K., Yi, J., 2004. Synthesis and characterization of mesoporous alumina with nickel incorporated for use in the partial oxidation of methane into synthesis gas. Appl. Catal. A. Gen. 272, 157–166.

Ko, J.D., Lee, J.K., Park, D., Shin, S.H., 1995. Kinetics of steam reforming over a Ni/alumina catalyst. Kor. J. Chem. Eng. 12, 478–480.

Lee, K.J., Park, D., 1998. Hydrogen production from fluidized bed steam reforming of hydrocarbons. Kor. J. Chem. Eng. 15, 658–662.

Lokurlu, A., Grube, T., Hohlein, B., Stolten, D., 2003. Fuel cells for mobile and stationary applications – cost analysis for combined heat and power stations on the basis of fuel cells. Int. J. Hydrogen Energy 28 (7), 703–711.

Løvik, I., 2011. Modelling, Estimation and Optimization of the Methanol Synthesis with Catalyst Deactivation. Norwegian University of Science and Technology.

Luna, A.E.C., Iriarte, M.E., 2008. Carbon dioxide reforming of methane over a metal modified Ni–Al_2O_3 catalyst. Appl. Catal. A. Gen. 343, 10–15.

Mallens, E.P.J., Hoebink, J.H.B.J., Marin, G.B., 1997. The reaction mechanism of the partial oxidation of methane to synthesis gas: a transient kinetic study over rhodium and a comparison with platinum. J. Catal. 167, 43–56.

Mark, M.F., Maier, W.F., Mark, F., 1997. Reaction kinetics of the CO_2 reforming of methane. Chem. Eng. Technol. 20, 361–370.

Muller-Langer, F., Tzimas, E., Kaltschmidtt, M., Peteves, S., 2007. Techno-economic assessment of hydrogen production processes for the hydrogen economy for the short and medium term. Int. J. Hydrogen Energy 32, 3797–3810.

Nakagawa, K., Anzai, K., Matsui, N., Ikenaga, N., Suzuki, T., Teng, Y., Kobayashi, T., Haruta, M., 1998. Effect of support on the conversion of methane to synthesis gas over supported iridium catalysts. Catal. Lett. 51, 163–167.

Nandini, A., Pant, K.K., Dhingra, S.C., 2006. Kinetic study of the catalytic carbon dioxide reforming of methane to synthesis gas over Ni–K/CeO_2–Al_2O_3 catalyst. Appl. Catal. A. Gen. 308, 119–127.
Nawaz, Z., Wei, F., 2011. Pt–Sn-based catalyst's intensification using Al_2O_3–SAPO-34 as a support for propane dehydrogenation to propylene. J. Ind. Eng. Chem. 17, 389–393.
Patel, K.S., Sunol, A.K., 2007. Modeling and simulation of methane steam reforming in a thermally coupled membrane reactor. Int. J. Hydrogen Energy 32, 2344–2358.
Rahimpour, M.R., Alizadehhesari, K., 2009. Enhancement of carbon dioxide removal in a hydrogen-permselective methanol synthesis reactor. Int. J. Hydrogen Energy 34, 1349–1362.
Rahimpour, M.R., Bayat, M., Rahmani, F., 2010. Enhancement of methanol production in a novel cascading fluidized-bed hydrogen permselective membrane methanol reactor. Chem. Eng. J. 157, 520–529.
Rahimpour, M.R., Rahmani, F., Bayat, M., Pourazadi, E., 2011. Enhancement of simultaneous hydrogen production and methanol synthesis in thermally coupled double-membrane reactor. Int. J. Hydrogen Energy 36, 284–298.
Rahimpour, M.R., Arab Aboosadi, Z., Jahanmiri, A.H., 2013a. Differential evolution (DE) strategy for optimization of methane steam reforming and hydrogenation of nitrobenzene in a hydrogen perm-selective membrane thermally coupled reactor. Int. J. Energy Res. 37 (8), 868–878.
Rahimpour, M.R., Farniaei, M., Abbasi, M., Javanmardi, J., Kabiri, S., 2013b. A comparative study on simultaneous production of methanol, hydrogen and DME using novel integrated thermally double coupled reactor. Energy Fuel 27 (4), 1982–1993.
Rahimpour, M.R., Hesami, M., Saidi, M., Jahanmiri, A., Farniaei, M., Abbasi, M., 2013c. Methane steam reforming thermally coupled with fuel combustion: application of chemical looping concept as a novel technology. Energy Fuel 27, 2351–2362.
Rostrup-Nielsen, J.R., 1993. Production of synthesis gas. Catal. Today 18, 305–324.
Ruckenstein, E., Hu, Y.H., 1998. Combination of CO_2 reforming and partial oxidation of methane over NiO/MgO solid solution catalysts. Ind. Eng. Chem. Res. 37, 1744–1747.
Ryden, M., Lyngfelt, A., Mattisson, T., 2006. Two novel approaches for hydrogen production; chemical-looping reforming and steam reforming with carbon dioxide capture by chemical looping combustion. WHEC 16, 13–16.
Ryden, M., Lyngfelt, A., 2006. Using steam reforming to produce hydrogen with carbon dioxide capture by chemical-looping combustion. Int. J. Hydrogen Energy 31, 1271–1283.
Sahebdelfar, S., Takht Ravanchi, M., Tahriri Zangeneh, F., Mehrazma, S., Rajabi, S., 2012. Kinetic study of propane dehydrogenation and side reactions over Pt–Sn/Al_2O_3 catalyst. Chem. Eng. Res. Des. 90, 1090–1097.
Samimi, F., Kabiri, S., Mirvakili, A., Rahimpour, M.R., 2013. The concept of integrated thermally double coupled reactor for simultaneous production of methanol, hydrogen and gasoline via differential evolution method. J. Nat. Gas Sci. Eng. 14, 144–157.
Seo, J.G., Youn, M.H., Cho, K.M., Park, S., Lee, S.H., Lee, J., et al., 2008a. Effect of Al_2O_3–ZrO_2 xerogel support on the hydrogen production by steam reforming of LNG over Ni/Al_2O_3–ZrO_2 catalyst. Kor. J. Chem. Eng. 25, 41–45.
Seo, J.G., Youn, M.H., Park, S., Lee, J., Lee, S.H., Lee, H., et al., 2008b. Hydrogen production by steam reforming of LNG over Ni/Al_2O_3–ZrO_2 catalysts: effect of ZrO_2 and preparation method of Al_2O_3–ZrO_2. Kor. J. Chem. Eng. 25, 95–98.
Simpson, A.P., Lutz, A.E., 2007. Exergy analysis of hydrogen production via steam methane reforming. Int. J. Hydrogen Energy 32, 4811–4820.
Song, C., 2001. Tri-reforming: a new process for reducing CO_2 emissions. Chem. Innov. 31 (1), 21–26.
Song, K.S., Seo, Y.S., Yoon, H.Y., Cho, S.J., 2003. Characteristics of the NiO/hexaaluminate for chemical looping combustion. Kor. J. Chem. Eng. 20, 471–475.
Sun, Z., Liu, F., Lin, X., Sun, B., Sun, D., 2012. Research and development of hydrogen fueled engines in China. Int. J. Hydrogen Energy 37, 664–681.
Takeguchi, T., Furukawa, S.N., Inoue, M., Eguchi, K., 2003. Autothermal reforming of methane over Ni catalysts supported over CaO–CeO_2–ZrO_2 solid solution. Appl. Catal. A. Gen. 240, 223–233.
Thapliyal, S., Deo, G., 2003. Propane dehydrogenation over alumina supported chromia catalysts. Bull. Chem. Soc. India 2, 29–33.
Tugnoli, A., Landucci, G., Cozzani, V., 2008. Sustainability assessment of hydrogen production by steam reforming. Int. J. Hydrogen Energy 33, 4345–4357.
Tullo, A.H., 2003. Engineering polymers. Chem. Eng. News 81, 21–25.
Vakili, R., Pourazadi, E., Setoodeh, P., Eslamloueyan, R., Rahimpour, M.R., 2011. Direct dimethyl ether (DME) synthesis through a thermally coupled heat exchanger reactor. Appl. Energy 88, 1211–1223.
Ventura, C., Azevedo, J.L.T., 2010. Development of a numerical model for natural gas steam reforming and coupling with a furnace model. Int. J. Hydrogen Energy 35, 9776–9787.
Vitry, D., Dubois, J.J., Ueda, W., 2004. Strategy in achieving propane selective oxidation over multi-functional Mo-based oxide catalysts. J. Mol. Catal. A. Chem. 220, 67–76.
Wang, Y., Wang, W., Hong, X., Li, Y., Zhang, Z., 2009. Yttrium-stabilized zirconia-promoted metallic nickel catalysts for the partial oxidation of methane to hydrogen. Int. J. Hydrogen Energy 34, 2252–2259.
Warren, B.K., Oyama, S.T., 1996. Heterogeneous Hydrocarbon Oxidation, vol. 638. Am. Chem. Soc.
Xu, G., Li, P., Rodrigues, A., 2002. Sorption enhanced reaction process with reactive regeneration. Chem. Eng. Sci. 57, 3893–3908.
Xu, J., Froment, G., 1989. Methane steam reforming, methanation and water gas shift: I. Intrinsic kinetics. AIChE J. 35, 88–96.
Youn, M.H., Seo, J.G., Cho, K.M., Jung, J.C., Kim, H., La, K.W., et al., 2008a. Effect of support on hydrogen production by auto-thermal reforming of ethanol over supported nickel catalysts. Kor. J. Chem. Eng. 25, 236–238.
Youn, M.H., Seo, J.G., Park, S., Jung, J.C., Park, D.R., Song, I.K., 2008b. Hydrogen production by auto-thermal reforming of ethanol over Ni catalysts supported on ZrO_2: effect of preparation method of ZrO_2 support. Int. J. Hydrogen Energy 33, 7457–7463.
Yu, C.Y., Lee, D.W., Park, S.J., Lee, K.Y., Lee, K.H., 2009. Study on a catalytic membrane reactor for hydrogen production from ethanol steam reforming. Int. J. Hydrogen Energy 34, 2947–2954.